

Conserved number fluctuations in a hadron resonance gas model

P. Garg^a, D. K. Mishra^b, P. K. Netrakanti^b, B. Mohanty^c, A. K. Mohanty^b, B. K. Singh^a, N. Xu^{d,e}

^a Department of Physics, Banaras Hindu University, Varanasi 221005, India

^b Nuclear Physics Division, Bhabha Atomic Research Center, Mumbai 400085, India

^c School of Physical Sciences, National Institute of Science Education and Research, Bhubaneswar 751005, India

^d Nuclear Science Division, Lawrence Berkeley National Laboratory, Berkeley, CA 94720, USA

^e Key Laboratory of the Ministry of Education of China, Central China Normal University, Wuhan, 430079, China

Abstract

Net-baryon, net-charge and net-strangeness number fluctuations in high energy heavy-ion collisions are discussed within the framework of a hadron resonance gas (HRG) model. Ratios of the conserved number susceptibilities calculated in HRG are being compared to the corresponding experimental measurements to extract information about the freeze-out condition and the phase structure of systems with strong interactions. We emphasize the importance of considering the actual experimental acceptances in terms of kinematics (pseudorapidity (η) and transverse momentum (p_T)), the detected charge state, effect of collective motion of particles in the system and the resonance decay contributions before comparisons are made to the theoretical calculations. In this work, based on HRG model, we report that the net-baryon number fluctuations are least affected by experimental acceptances compared to the net-charge and net-strangeness number fluctuations.

Keywords: , Hadron Resonance Gas, Susceptibilities, Higher moments, Fluctuations, Heavy-ion collisions, Critical point
PACS: 25.75.Bh, 25.75.Ld

1. Introduction

Measurement of the moments of distribution for conserved quantities like net-baryon, net-charge and net-strangeness number for systems undergoing strong interactions as in high energy heavy-ion collisions, have recently provided rich physics insights [1, 2, 3, 4, 5, 6, 7, 8, 9, 10]. The most crucial realization is that, the product of moments of the conserved number distributions are measurable experimentally and can be linked to susceptibilities (χ) computed in Quantum Chromodynamic (QCD) based calculations [1, 5]. For example, $S\sigma = \chi^{(3)}/\chi^{(2)}$ and $\kappa\sigma^2 = \chi^{(4)}/\chi^{(2)}$, where σ is the standard deviation, S is the skewness, κ is the kurtosis of the measured conserved number distribution, $\chi^{(n)}$ are the n^{th} order theoretically calculated susceptibilities associated with these conserved numbers. Such a connection between theory and high energy heavy-ion collision experiment has led to furthering our understanding about the freeze-out conditions [2, 4], details of the quark-hadron transition [1, 8] and plays a crucial role for the search of possible QCD critical point in the QCD phase diagram [5]. In all such physics cases there is a need to establish a reference point for the measurements. Computing these quantities within the framework of a hadron resonance gas (HRG) model [11] provides such a reference for both experimental data and QCD based calculations.

The experimental measurements have limitations, they are usually available for a fraction of the total kinematic phase space, due to the finite detector geometries and can detect

only certain species of the produced particles. For example, measurements related to net-baryon number distribution is restricted by the kinematic range in p_T where their identification is possible. In addition, baryons like neutron are not commonly measured in most of the high energy heavy-ion collision experiments. While for the net-charge number distribution, the limitation is usually in kinematic range available in η and the details of how contribution from different charge states and resonances are dealt with in the measurements. The kinematic acceptance in a typical high energy heavy-ion collision experiment like STAR [12] and PHENIX [13] at the Relativistic Heavy-Ion Collider facility (RHIC) for net-charge multiplicity distributions are: $|\eta| < 0.5$, $0.2 < p_T < 2.0$ GeV/c and $|\eta| < 0.35$, $0.3 < p_T < 1.0$ GeV/c, respectively. While for net-baryon number and net-strangeness related studies carried out in the STAR experiment, within $|\eta| < 0.5$, is through the measurement of net-protons and net-kaons in the range of $0.4 < p_T < 0.8$ GeV/c and $0.2 < p_T < 2.0$ GeV/c, respectively [5, 12].

The main goal of this paper is to demonstrate using the HRG model (discussed in next section), the effect of the above experimental limitations on the physics observables $\chi^{(3)}/\chi^{(2)}$ and $\chi^{(4)}/\chi^{(2)}$. Our model based study clearly shows that the value of the observables related to net-charge and net-strangeness strongly depends on the experimental kinematic and charge state acceptances. Where charge state could be electric charge (Q) = 1 or higher for net-charge measurements and strangeness number (S) = 1 or higher for net-strangeness measurements. In contrast, the net-baryon number studies are found to be minimally affected by these experimental limitations. In this work, we have not considered the initial baryon distribution due to the

Email address: bedanga@rcf.rhic.bnl.gov (B. Mohanty)

participant number fluctuations in the heavy-ion collisions on the results for net-baryon fluctuations [14]. Another important effect that could influence the values of the higher moments of the net-charge, net-strangeness and net-baryon number distributions in limited acceptance, are the conservation laws related to charge, strangeness and baryon number.

The paper is organized as follows. In the Section 2, we will discuss the HRG model used in this study. In the Section 3, the results for the observable $\chi^{(3)}/\chi^{(2)}$ and $\chi^{(4)}/\chi^{(2)}$ are presented for different kinematic acceptances, charge states, effect of collective flow of particle in the system and the resonance decay contributions. We also provide a table listing the values of these observable for typical experimental conditions as encountered in STAR and PHENIX experiments at RHIC and ALICE experiment at the Large Hadron Collider (LHC) Facility. Finally in Section 4, we summarize our findings and mention about the implications of this work to the current experimental measurements in high energy heavy-ion collisions.

2. Hadron Resonance Gas Model

In the HRG model, we include all the relevant degrees of freedom of the confined, strongly interacting matter and also implicitly take into account the interactions that result in resonance formation [3]. It is well known that the fireball created in heavy ion collision does not remain static, rather expands both in longitudinal and transverse directions until freeze out occurs. However, to keep the model simple, we first consider a static homogeneous fireball and flow effects are included subsequently.

In heavy ion collision, no fluctuation would be seen in measurements with full phase space coverage as B , Q and S are strictly conserved. However, since most of the experiments cover only limited phase space, the part of the fireball accessible to the measurements may resemble with the Grand Canonical Ensemble (GCE) where energy (momentum), charge and number are not conserved locally. In general, the magnitude of multiplicity fluctuations and correlations in limited phase space crucially depends on the choice of the statistical ensemble that imposes different conservation laws [15, 16]. Since no extensive quantities like energy, momentum and charge are needed to be locally conserved in GCE, the particles following Maxwell-Boltzmann distribution are assumed to be uncorrelated and fluctuations are expected to follow Poisson statistics even in the limited phase space when quantum effects are ignored. In case of particles following Bose-Einstein or Fermi-Dirac distributions, within finite phase space, Poisson statistics is not expected to be obeyed and hence the deviations from Poisson limit can be studied.

In the ambit of GCE framework, the logarithm of the partition function (Z) in the HRG model is given as,

$$\ln Z(T, V, \mu) = \sum_B \ln Z_i(T, V, \mu_i) + \sum_M \ln Z_i(T, V, \mu_i), \quad (1)$$

where,

$$\ln Z_i(T, V, \mu_i) = \pm \frac{V g_i}{2\pi^2} \int d^3 p \ln \{1 \pm \exp[(\mu_i - E)/T]\}, \quad (2)$$

T is the temperature, V is the volume of the system, μ_i is the chemical potential, E is the energy and g_i is the degeneracy factor of the i^{th} particle. The total chemical potential $\mu_i = B_i \mu_B + Q_i \mu_Q + S_i \mu_S$, where B_i , Q_i and S_i are the baryon, electric charge and strangeness number of the i^{th} particle, with corresponding chemical potentials μ_B , μ_Q and μ_S , respectively. The '+' and '-' signs are for baryons and mesons respectively. The thermodynamic pressure (P) can then be deduced for the limit of large volume as

$$\frac{P}{T^4} = \frac{1}{VT^3} \ln Z_i = \pm \frac{g_i}{2\pi^2 T^3} \int d^3 p \ln \{1 \pm \exp[(\mu_i - E)/T]\}. \quad (3)$$

The n^{th} order generalized susceptibility for baryons can be expressed as [3],

$$\chi_{x,baryon}^{(n)} = \frac{X^n}{VT^3} \int d^3 p \sum_{k=0}^{\infty} (-1)^k (k+1)^n \exp\left\{\frac{-(k+1)E}{T}\right\} \exp\left\{\frac{(k+1)\mu}{T}\right\}, \quad (4)$$

and for mesons,

$$\chi_{x,meson}^{(n)} = \frac{X^n}{VT^3} \int d^3 p \sum_{k=0}^{\infty} (k+1)^n \exp\left\{\frac{-(k+1)E}{T}\right\} \exp\left\{\frac{(k+1)\mu}{T}\right\}. \quad (5)$$

The factor X represents either B , Q or S of the i^{th} particle depending on whether the computed χ_x represents baryon or electric charge or strangeness susceptibility.

For a particle of mass m in static fireball with p_T , η and ϕ (azimuthal angle), the volume element ($d^3 p$) and energy (E) can be written as $d^3 p = p_T m_T \cosh \eta dp_T d\eta d\phi$ and $E = m_T \cosh \eta$, where $m_T = \sqrt{p_T^2 + m^2}$, respectively. The experimental acceptances can be incorporated by considering the appropriate integration ranges in η , p_T , ϕ and charge states by considering the values of $|X|$. The total generalized susceptibilities will then be the sum of the contribution from baryons and mesons as, $\chi_x^{(n)} = \sum \chi_{x,baryon}^{(n)} + \sum \chi_{x,meson}^{(n)}$.

In order to make the connection with the experiments, the beam energy dependence of μ and T parameters of the HRG model needs to be provided. These are extracted from a statistical thermal model description of measured particle yields in the experiment at various $\sqrt{s_{NN}}$ [17, 18, 19]. This is followed by the parameterization of μ_B and T as a function of $\sqrt{s_{NN}}$ [17]. The μ_B dependence of the temperature is given as $T(\mu_B) = a - b\mu_B^2 - c\mu_B^4$ with $a = 0.166 \pm 0.002$ GeV, $b = 0.139 \pm 0.016$ GeV $^{-1}$, and $c = 0.053 \pm 0.021$ GeV $^{-3}$. The $\sqrt{s_{NN}}$ dependence of μ_B is given as $\mu_B(\sqrt{s_{NN}}) = \frac{d}{1+e\sqrt{s_{NN}}}$ with $d = (1.308 \pm 0.028)$ GeV and $e = (0.273 \pm 0.008)$ GeV $^{-1}$. Further the ratio of baryon to strangeness chemical potential is parameterized as $\frac{\mu_S}{\mu_B} \simeq 0.164 + 0.018 \sqrt{s_{NN}}$. We have checked that the value of T and μ_B obtained using the yields extrapolated to 4π or from mid-rapidity measurements, have little impact on our study. However in order to study the rapidity (η) dependence, the μ_B parameterizations $\mu_B = 0.024 + 0.011\eta^2$

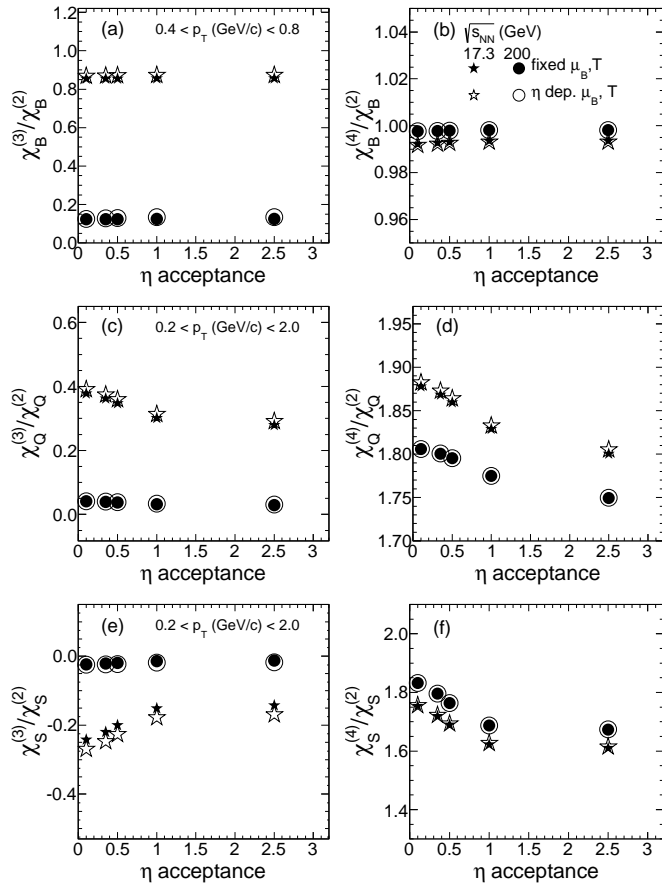


Figure 1: The η acceptance dependence of $\chi_x^{(3)}/\chi_x^{(2)}$ and $\chi_x^{(4)}/\chi_x^{(2)}$ for two different beam energies. In panel (a) and (b) x = net-baryon B , (c) and (d) x = net-charge Q , and in (e) and (f) x = net-strangeness S . Also shown are the results with (labeled “dep.”) and without (labeled “fixed”) the η dependence of chemical freeze-out parameters μ_B and T .

and $\mu_B = 0.237 + 0.011\eta^2$ at $\sqrt{s_{NN}} = 200$ GeV [20] and $\sqrt{s_{NN}} = 17.3$ GeV [21], respectively are used in the calculations.

3. Results

3.1. Kinematic acceptance in η and p_T

Figure 1 shows the variation of $\chi_x^{(3)}/\chi_x^{(2)}$ and $\chi_x^{(4)}/\chi_x^{(2)}$ as a function of η acceptance for $\sqrt{s_{NN}} = 200$ GeV and $\sqrt{s_{NN}} = 17.3$ GeV. Where x stands for either net-baryon (B) (Fig. 1 (a) and (b)), net-charge (Q) (Fig. 1 (c) and (d)), or net-strangeness (S) (Fig. 1 (e) and (f)). For each beam energy we show the effect of considering HRG parameters (μ , T) fixed to parameterization based on mid-rapidity data and also a parameterization based on the η dependent value of (μ , T). The difference between the two cases are small. For the subsequent studies we only present results for different $\sqrt{s_{NN}}$ using the parameterization of the chemical freeze-out parameters based on the measurement of particle yields at mid-rapidity. A clear dependence of $\chi_x^{(3)}/\chi_x^{(2)}$ and $\chi_x^{(4)}/\chi_x^{(2)}$ on η acceptance is observed for net-charge (Fig. 1 (c) and (d)) and net-strangeness (Fig. 1 (e) and (f)). The $\chi_B^{(3)}/\chi_B^{(2)}$ and $\chi_B^{(4)}/\chi_B^{(2)}$ values (Fig. 1 (a) and

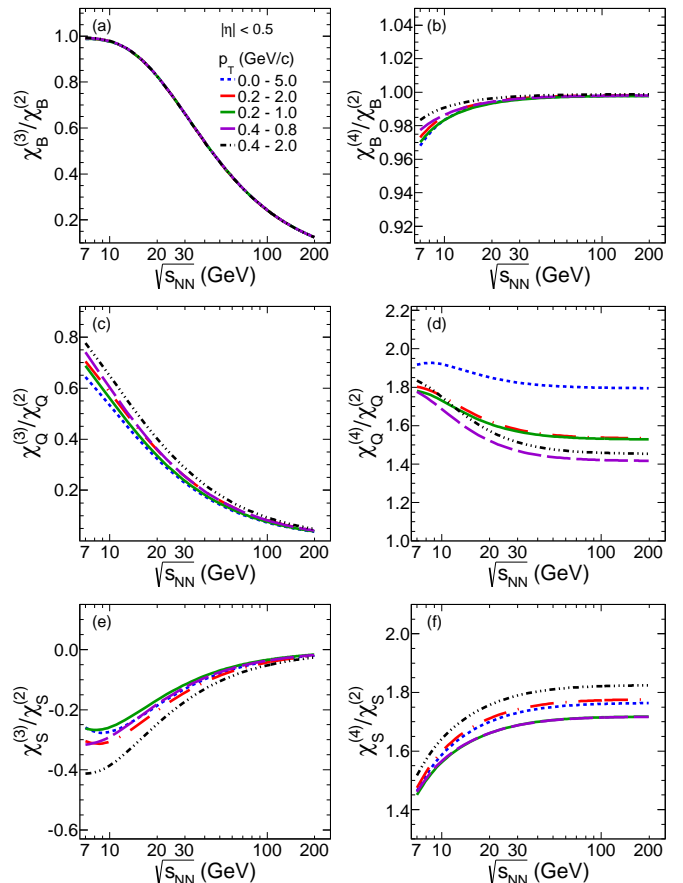


Figure 2: (Color online) The p_T acceptance dependence of $\chi_x^{(3)}/\chi_x^{(2)}$ and $\chi_x^{(4)}/\chi_x^{(2)}$ for different $\sqrt{s_{NN}}$. Where x stands for either net-baryon (B) (panels (a) and (b)), net-charge (Q) (panels (c) and (d)), and net-strangeness (S) (panels (e) and (f)).

(b)) are however found to be independent of η acceptance for the two beam energies studied. This underscores the need to carefully consider η acceptance effects when comparing HRG model results to experimental data, especially for net-charge and net-strangeness fluctuation measures.

Figure 2 shows the variation of $\chi_x^{(3)}/\chi_x^{(2)}$ and $\chi_x^{(4)}/\chi_x^{(2)}$ as a function of $\sqrt{s_{NN}}$ for various p_T acceptances. The choice of these particular values of p_T acceptance ranges are motivated by existence of the corresponding experimental measurements [5, 12, 13]. It is observed that $\chi_x^{(3)}/\chi_x^{(2)}$ and $\chi_x^{(4)}/\chi_x^{(2)}$ have a clear p_T acceptance dependence at all beam energies for net-charge (Fig. 2 (c) and (d)) and net-strangeness (Fig. 2 (e) and (f)). However the p_T acceptance dependences for net-baryon (Fig. 2 (a) and (b)) is substantially weaker. Hence the p_T acceptance study also emphasizes the need to consider the actual experimental acceptance for model comparisons in fluctuation measures. At the same time both the kinematic acceptance studies in η and p_T show net-baryon fluctuation measures are least affected.

3.2. Conserved charge states

Figure 3 shows the variation of $\chi_x^{(3)}/\chi_x^{(2)}$ and $\chi_x^{(4)}/\chi_x^{(2)}$ as a function of $\sqrt{s_{NN}}$ for various types of baryons (Fig. 3 (a) and

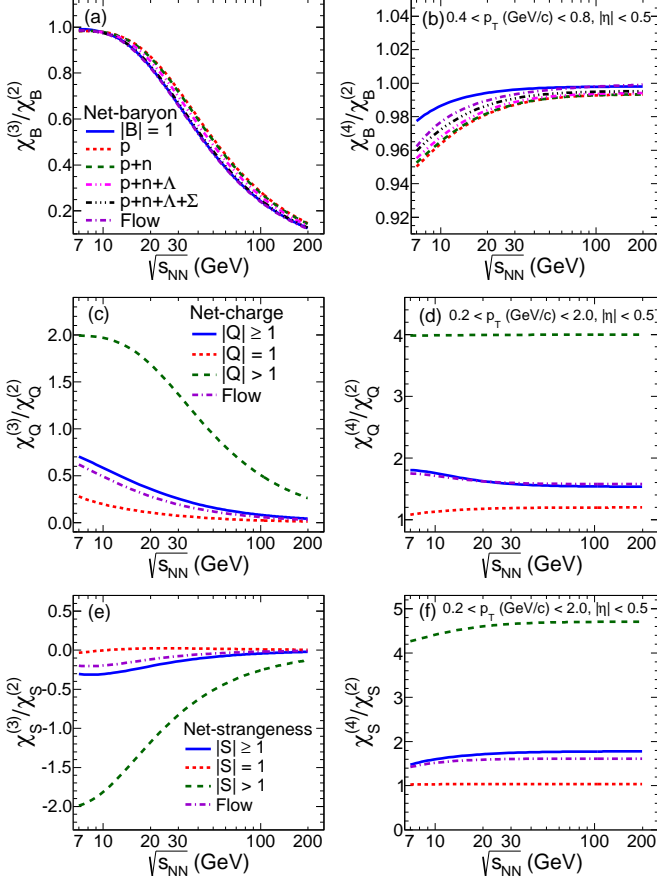


Figure 3: (Color online) The variation of $\chi_x^{(3)}/\chi_x^{(2)}$ and $\chi_x^{(4)}/\chi_x^{(2)}$ for net-baryon (B), net-charge (Q), and net-strangeness (S) as a function of collision energy ($\sqrt{s_{NN}}$). The results are shown for different baryons (panels (a) and (b)), electric charge states (panels (c) and (d)) and strangeness number (panels (e) and (f)) considered in the calculation.

(b)), values of electric charge states, $|Q| = 1$ and $|Q| > 1$ (Fig. 3 (c) and (d)), and values of strangeness number, $|S| = 1$ and $|S| > 1$ (Fig. 3 (e) and (f)). For each of the cases the observables are compared to the respective values with inclusion of all conserved charge states and baryons. We find a strong dependence of the $\chi_Q^{(3)}/\chi_Q^{(2)}$ and $\chi_Q^{(4)}/\chi_Q^{(2)}$ on whether we consider $|Q| = 1$ or $|Q| > 1$, both differing from the case of inclusion of all charge states. Same is the situation for net-strangeness. On the other hand, successive inclusion of different baryons, starting with protons seems to have some small effect on the $\chi_B^{(3)}/\chi_B^{(2)}$ and $\chi_B^{(4)}/\chi_B^{(2)}$ values only at the lower beam energies. The absence of baryons with $|B| > 1$ makes the net-baryon number fluctuations more advantageous and less prone to kinematic acceptances as compared to the net-charge or net-strangeness fluctuation measures.

3.3. Effect of flow

To study the effect of flow on the ratios of susceptibilities in the HRG model, we now consider an expanding fireball with four velocity,

$$u^\mu = \text{cosh}_T(\text{cosh}y_0, \tanh y_T, 0, \sinh y_0), \quad (6)$$

where y_0 is the longitudinal and $y_T = \tanh^{-1}(\beta_r)$ is the transverse rapidity of the fireball flowing with radial flow velocity β_r . The four-momentum of the particle can be expressed as:

$$p^\mu = (m_T \cosh \eta, p_T \cos \phi, p_T \sin \phi, m_T \sinh \eta) \quad (7)$$

In the presence of flow, the logarithm of the partition function for i^{th} particle having four momentum p^μ can be expressed as,

$$\ln Z_i(T, V, \mu_i) = \pm \frac{g_i}{(2\pi)^3} \int_\sigma d^3 p \frac{p^\mu d\sigma_\mu}{p^0} \ln \{1 \pm \exp[(\mu_i - p^\mu u_\mu)/T]\}, \quad (8)$$

where σ represents the space-time surface whose surface elements can be represented by four vector denoted by $d\sigma_\mu$ and p^0 is the energy of the particle. Assuming instantaneous freeze out (at time τ_f) in the radial direction r , $p^\mu d\sigma_\mu$ simplifies as [22],

$$p^\mu d\sigma_\mu = \tau_f r dr d\phi dy_0 m_T \cosh(\eta - y_0). \quad (9)$$

The limit of integration for r varies from 0 to R_f (freeze out radius), ϕ from 0 to 2π , y_0 from $-y_0^{\text{min}}$ to y_0^{max} ($= \ln(\sqrt{s_{NN}}/m_p)$, where m_p is mass of proton). The other variables p_T and η vary within the experimental acceptances. Note that we recover eq. 2 for the case of static fireball ($y_T = y_0 = 0$) where $p^\mu u_\mu = E$ and the integral over $(p^\mu d\sigma_\mu)/p^0$ becomes proportional to $4\pi V$. Therefore, for a constant β_r , the flow effect on the susceptibilities can be incorporated by replacing $d^3 p$ integral in eq. 4 and eq. 5 with $p_T dp_T d\eta d\phi dy_0 m_T \cosh(\eta - y_0)$ and the energy E in the exponentials by the invariant $p^\mu u_\mu$ as defined above. Further, under the assumption that the flow velocity β_r is independent of radial position, the r integration turns out to be a constant which is proportional to the volume at freeze-out. For the simplicity of the calculations, we have used a constant β_r (same as β_s of ref [23]). Figure 3 also shows the effect of flow (longitudinal + transverse) on the ratios of susceptibilities as a function of collision energy. It is noticed that the ratios of the susceptibilities like $\chi_x^{(4)}/\chi_x^{(2)}$ for net-baryon, net-charge and net-strangeness are affected by less than (2 - 4)% as compared to the corresponding static values represented by solid blue line.

3.4. Resonance decay

The generalized susceptibility of n^{th} order can be written as,

$$\chi^n = \sum_p \chi_p^n + \sum_R \epsilon_R^n \chi_R^n, \quad (10)$$

where χ_p^n and χ_R^n are the contributions to the n^{th} order susceptibility due to primordial and resonance yields respectively. The factor ϵ_R^n is an event averaged efficiency at which resonance R contributes to the generalized susceptibility. Note that $\epsilon_R^n = 1$ when all the decay particles are fully accepted and $\epsilon_R^n < 1$ due to finite detector and kinematic acceptances. Consider the example of the resonance Δ^{++} which decays into p and π^+ with branching ratio b . Using a toy Monte Carlo simulation, we generate Δ^{++} distribution with Poisson statistics and build the charge distributions both for Δ^{++} and the decay particles (proton and pion together) within the experimental acceptances. The Poisson distribution for Δ^{++} is a reasonable assumption

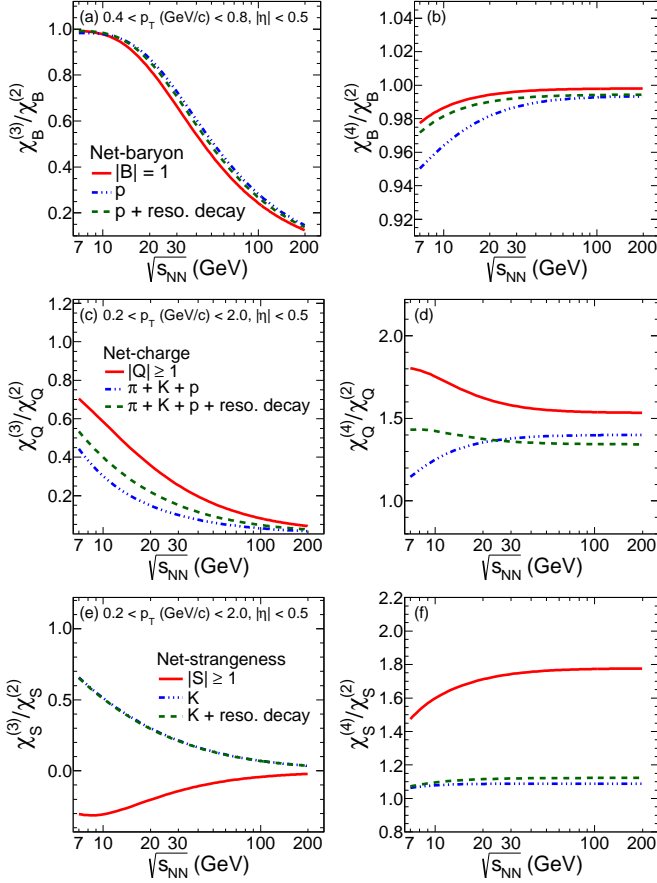


Figure 4: (Color online) The variation of $\chi_x^{(3)}/\chi_x^{(2)}$ and $\chi_x^{(4)}/\chi_x^{(2)}$ for net-baryon (B), net-charge (Q), and net-strangeness (S) with different beam energies ($\sqrt{s_{NN}}$) with and without resonance decay daughter particle acceptance effects.

as momentum distributions of resonance particles can be approximated by the classical Maxwell-Boltzmann function due to their large masses, although it is not true for their decay products. Therefore, we estimate the efficiency ϵ^n by taking the ratios of the n^{th} order cumulant of the charge distributions after and before decays. Similar procedures are adopted for other resonances to estimate the average efficiencies ϵ_R^n depending on the charge, strangeness and baryon number as appropriate.

The results of $\chi_x^{(3)}/\chi_x^{(2)}$ and $\chi_x^{(4)}/\chi_x^{(2)}$ with and without considering the effect of resonance daughter particle acceptances are shown in Fig. 4. In Fig. 4(a) and (b), three cases for $\chi_B^{(3)}/\chi_B^{(2)}$ and $\chi_B^{(4)}/\chi_B^{(2)}$ are shown within a realistic acceptance of $|\eta| < 0.5$ and $0.4 < p_T < 0.8$ GeV/c. The results for all baryons without any resonance decay (solid red curve), results for protons without any resonance decay contribution (dotted blue curve) and results for protons with resonance decay (dashed green curve). Similarly in Fig. 4(c) and (d) shows $\chi_Q^{(3)}/\chi_Q^{(2)}$ and $\chi_Q^{(4)}/\chi_Q^{(2)}$ respectively, for all charges without resonance decay (solid red curve), pions, kaons and protons without resonance decay (dotted blue curve) and pions, kaons and protons with resonance decay (dashed green curve). Fig. 4(e) and (f), are shown the results for all strangeness without resonance decay (solid red curve), kaons without resonance decay (dotted blue curve) and

kaons with resonance decay (dashed green curve).

It may be mentioned here that the efficiency ϵ_R^n is an event averaged quantity and will have fluctuations on an event by event basis. Although ϵ_R^n has inherent fluctuation, a rough estimate shows that it's effect on the ratio of $\chi_Q^{(4)}/\chi_Q^{(2)}$ is $\sim 2\%$ which we have ignored in the present study. Therefore, the present estimate of the effect of resonance decays on the ratio of susceptibilities are approximate. Nevertheless, it brings out the importance of resonance decays which certainly affect all the ratios. With these assumption, the effects of resonance decay due to finite experimental acceptances are large for net-charge and net-strangeness as compared to net-baryons. The acceptance used in this study are modest and are close to the present experimental acceptances.

Through our work we have emphasized the need for considering experimental acceptances of various kinds in model, such as HRG, before they are considered to provide the baseline to experimental measurements for drawing physics conclusions. Hence in the Tables 1, 2, 3 and 4 we provide values of $\chi_x^{(3)}/\chi_x^{(2)}$ and $\chi_x^{(4)}/\chi_x^{(2)}$ for typical ongoing experimental acceptances. The values quoted in the tables are for static fireball and without including the resonance decay products. The $\chi_Q^{(3)}/\chi_Q^{(2)}$ and $\chi_Q^{(4)}/\chi_Q^{(2)}$ values are provided for two typical acceptances $|\eta| < 0.5$, $0.2 < p_T < 2.0$ GeV/c and $|\eta| < 0.35$, $0.3 < p_T < 1.0$ GeV/c (Table 1 and Table 2). The $\chi_S^{(3)}/\chi_S^{(2)}$ and $\chi_S^{(4)}/\chi_S^{(2)}$ are provided for a typical acceptance of $|\eta| < 0.5$, $0.2 < p_T < 2.0$ GeV/c (Table 3). The $\chi_B^{(3)}/\chi_B^{(2)}$ and $\chi_B^{(4)}/\chi_B^{(2)}$ are provided for a typical acceptance of $|\eta| < 0.5$, $0.4 < p_T < 0.8$ GeV/c (Table 4).

Table 1: Ratios of the moments for net-charge within $|\eta| < 0.5$, and $0.2 < p_T < 2.0$ GeV/c.

$\sqrt{s_{NN}}$ (GeV)	$\chi_Q^{(3)}/\chi_Q^{(2)}$	$\chi_Q^{(4)}/\chi_Q^{(2)}$
5	0.526	1.413
7.7	0.414	1.430
11.5	0.321	1.407
15	0.265	1.390
19.6	0.215	1.375
27	0.165	1.361
39	0.119	1.352
62.4	0.077	1.346
130	0.038	1.343
200	0.025	1.342
2760	0.002	1.341

4. Summary

In summary, using a hadron resonance gas model we have studied the effect of limited experimental acceptance on observables like n^{th} order susceptibilities $\chi_x^{(n)}$, associated with conserved quantities like net-charge ($x = Q$), net-strangeness ($x = S$) and net-baryon number ($x = B$). The various order susceptibilities which can also be calculated in QCD based models are related to the moments (σ , S and κ) of the corresponding measured conserved number distributions. These observ-

Table 2: Ratios of the moments for net-charge within $|\eta| < 0.35$, and $0.3 < p_T < 1.0$ GeV/c.

$\sqrt{s_{NN}}$ (GeV)	$\chi_Q^{(3)}/\chi_Q^{(2)}$	$\chi_Q^{(4)}/\chi_Q^{(2)}$
5	0.432	1.231
7.7	0.332	1.245
11.5	0.256	1.233
15	0.212	1.222
19.6	0.172	1.213
27	0.132	1.205
39	0.095	1.199
62.4	0.062	1.196
130	0.031	1.194
200	0.020	1.193
2760	0.001	1.193

Table 3: Ratios of the moments for net-kaon within $|\eta| < 0.5$, and $0.2 < p_T < 2.0$ GeV/c.

$\sqrt{s_{NN}}$ (GeV)	$\chi_K^{(3)}/\chi_K^{(2)}$	$\chi_K^{(4)}/\chi_K^{(2)}$
5	0.726	1.058
7.7	0.560	1.090
11.5	0.428	1.108
15	0.353	1.115
19.6	0.288	1.120
27	0.222	1.123
39	0.162	1.125
62.4	0.107	1.127
130	0.054	1.128
200	0.035	1.128
2760	0.003	1.128

ables have been widely used to understand the freeze-out conditions in heavy-ion collisions and various aspects of the phase structure of the QCD phase diagram. Our study demonstrates the importance of considering experimental acceptances of different kinds before measurements are compared to theoretical calculations, specifically in the use of HRG model as a baseline for such fluctuation based study. We observe finite kinematic acceptances in η and p_T have a strong effect on the $\chi_Q^{(n)}$ and $\chi_S^{(n)}$ values. These susceptibilities are also very sensitive to the accepted electric charge states and strangeness states in the experiment. However, the effect of flow is less than (2 - 4)% on the ratios of susceptibilities for net-baryon, net-charge and net-strangeness and the improvements can be done in implementation of the radial dependent transverse flow velocities. In addition, we find in this model that, the $\chi_Q^{(n)}$ and $\chi_S^{(n)}$ values depends on the experimental acceptance of the decay daughters from various resonances produced in high energy heavy-ion collisions. Within this model and the kinematic regions used in our study, we find that the dependence on acceptance and resonance decays are stronger for both net-charge and net-strangeness compared to that of net-baryons.

Acknowledgments We thank Sourendu Gupta for useful discussions related to this paper. BM is supported by the DST

Table 4: Ratios of the moments for net-proton within $|\eta| < 0.5$, and $0.4 < p_T < 0.8$ GeV/c.

$\sqrt{s_{NN}}$ (GeV)	$\chi_P^{(3)}/\chi_P^{(2)}$	$\chi_P^{(4)}/\chi_P^{(2)}$
5	0.981	0.961
7.7	0.987	0.975
11.5	0.962	0.984
15	0.920	0.988
19.6	0.851	0.991
27	0.737	0.993
39	0.586	0.995
62.4	0.407	0.996
130	0.210	0.997
200	0.139	0.997
2760	0.010	0.997

SwarnaJayanti project fellowship. PG acknowledges the financial support from CSIR, New Delhi, India.

References

- [1] S. Gupta, X. Luo, B. Mohanty, H. G. Ritter and N. Xu, *Science* **332** (2011) 1525.
- [2] R. V. Gavai and S. Gupta, *Phys. Lett. B* **696** (2011) 459.
- [3] F. Karsch and K. Redlich, *Phys. Lett. B* **695** (2011) 136.
- [4] A. Bazavov, H. T. Ding, P. Hegde, O. Kaczmarek, F. Karsch, E. Laermann, S. Mukherjee and P. Petreczky *et al.*, *Phys. Rev. Lett.* **109** (2012) 192302.
- [5] M. M. Aggarwal *et al.* [STAR Collaboration], *Phys. Rev. Lett.* **105** (2010) 022302.
- [6] M. A. Stephanov, *Phys. Rev. Lett.* **107** (2011) 052301.
- [7] P. Braun-Munzinger, B. Friman, F. Karsch, K. Redlich and V. Skokov, *Phys. Rev. C* **84** (2011) 064911.
- [8] B. Friman, F. Karsch, K. Redlich and V. Skokov, *Eur. Phys. J. C* **71** (2011) 1694.
- [9] C. B. Yang and X. Wang, *Phys. Rev. C* **84** (2011) 064908.
- [10] M. Asakawa, S. Ejiri and M. Kitazawa, *Phys. Rev. Lett.* **103** (2009) 262301.
- [11] P. Braun-Munzinger, K. Redlich and J. Stachel, In *Hwa, R.C. (ed.) *et al.*: Quark gluon plasma* 491-599 [nucl-th/0304013].
- [12] D. McDonald [STAR Collaboration], arXiv:1210.7023 [nucl-ex].
- [13] J. T. Mitchell [PHENIX Collaboration], arXiv:1211.6139 [nucl-ex].
- [14] V. P. Konchaovski, M. I. Gorenstein, E. L. Bratkovskaya and H. Stocker, *Phys. Rev. C* **74** (2006) 064911.
- [15] M. Hauer, G. Torrieri and S. Wheaton, *Phys. Rev. C* **80** (2009) 014907; M. Hauer, arXiv:1008.1990 and references there in.
- [16] M. Hauer, *Phys. Rev. C* **77** (2008) 034909.
- [17] J. Cleymans, H. Oeschler, K. Redlich and S. Wheaton, *Phys. Rev. C* **73** (2006) 034905 and references there in.
- [18] F. Becattini, M. Gazdzicki A. Keranen J. Manninen and R. Stock, *Phys. Rev. C* **69** (2004) 024905.
- [19] F. Becattini, J. Manninen and M. Gazdzicki, *Phys. Rev. C* **73** (2006) 044905.
- [20] J. Cleymans, *J. Phys. G: Nucl. Part. Phys.* **35** (2008) 044017.
- [21] F. Becattini, J. Cleymans and J. Strumpher, *PoS CPOD* **07** (2007) 012.
- [22] P. V. Ruuskanen, *Acta Physica Polonica B* **18** (1987) 551.
- [23] B. I. Abelev *et al.*, STAR Collaboration, *Phys. Rev. C* **79** (2009) 34909.